RSC Advances

PAPER

View Article Online
View Journal | View Issue

Cite this: *RSC Adv.*, 2025, **15**, 43737

Polyvinyl alcohol/organic montmorillonite composite coatings applied to paper-based barrier packaging materials

Zheng Cheng, *[abcde] Mei Ning,[acde] Xinmei Nong,[acde] Naiyu Xiao,[acde] Xueqin Zhang,[abcde] Le Zhong,[acde] Honglei Wang,*[abcde] Guojian Chen[acde] and Qianbin Mo[acde]

With the continuous improvement of global environmental awareness, the issue of white pollution caused by plastic packaging needs to be effectively solved. Nowadays, the application of sustainable packaging materials has become a developing trend in the packaging industry. In this study, montmorillonite (MMT) was modified to obtain organic montmorillonite (OMMT), which was then combined with polyvinyl alcohol (PVA), after which glycerol, tributyl phosphate, and sodium tetraborate were added to prepare PVA/OMMT composite coatings with high barrier properties, which were successfully coated onto Kraft paper *via* a facile automatic coating process. Results show that the modification process can optimize the overall properties of the PVA/OMMT composite coating and endow the coated paper with outstanding barrier performance. The oxygen permeability decreased to 14.92 $cm^3\ m^{-2}\cdot 24$ h Pa, and the water vapor transmission rate reduced to 2.68×10^{-12} g cm $cm^{-2}\ s^{-1}$ Pa. This was because sodium tetraborate reacted with PVA to form a stable borate ester bond, which enhanced the water resistance of the coated paper. The modified OMMT and sodium tetraborate were combined with PVA to effectively prevent gas permeation. Additionally, the composite coatings exhibited some oil resistance, enhancing the barrier effect of the Kraft paper. These findings suggested that PVA/OMMT-coated Kraft paper had both environmental protection and high barrier properties, offering an innovative approach to developing eco-friendly packaging materials and promoting the application of barrier coatings in paper-based packaging materials.

Received 21st August 2025
Accepted 2nd October 2025

DOI: 10.1039/d5ra06196b

rsc.li/rsc-advances

Introduction

Practicing a green, low-carbon lifestyle has become a hot topic of concern for society as a whole in recent years. Various industries, especially the packaging industry, have been paying increasing attention to environmental protection.[1,2] In this context, eco-packaging has become an important trend in the packaging industry. At the same time, the market demand for paper packaging is also increasing. Nevertheless, plastic packaging still dominates the market due to its lightweight design, good sealing, affordability, and other advantages. According to statistics,[3] global plastic consumption will range from 600 to 1000 million tons by 2050. Worryingly, the white pollution caused by plastic packaging is becoming increasingly serious and must be effectively addressed. At present, the use of sustainable packaging materials is a development trend in the packaging industry. Paper-based packaging, a fully environmentally friendly material, offers recyclability, light weight, ease of processing and molding, and other characteristics, and its unique environmental advantages make it an ideal alternative to plastic packaging.[4,5] However, the low-barrier properties of paper-based packaging can easily lead to a reduction in its mechanical properties under high humidity conditions, which limits its high-quality development.[6] This is because the structure of paper products, formed by crisscrossing fibers, contains many holes.[7] When there is a concentration difference between the two sides, small molecules (gas, water vapor, and grease) can diffuse from the side of higher concentration to the side of lower concentration, leading to poor barrier performance of the paper-based packaging material.[8] Therefore, one common way to improve the barrier performance of paper-based packaging is

[a]*College of Light Industry and Food Technology, Zhongkai University of Agriculture and Engineering, Guangzhou, CN 510225, China. E-mail: chengzheng@zhku.edu.cn; wanghonglei@zhku.edu.cn*

[b]*State Key Laboratory of Advanced Papermaking and Paper-based Materials, South China University of Technology, Guangzhou, CN 510640, China*

[c]*Guangdong Engineering Technology Research Center for Food Green Packaging, Zhongkai University of Agriculture and Engineering, Guangzhou, CN 510225, China*

[d]*Key Laboratory of Green Processing and Intelligent Manufacturing of Lingnan Specialty Food, Ministry of Agriculture and Rural Affairs, Zhongkai University of Agriculture and Engineering, Guangzhou 510225, China*

[e]*Guangdong Provincial Key Laboratory of Lingnan Specialty Food Science and Technology, Zhongkai University of Agriculture and Engineering, Guangzhou 510225, China*

to apply a high-barrier coating to its surface.[9,10] Barrier coating, a functional coating primarily applied to the packaging substrate, greatly reduces the permeation of small molecules through the substrate, thereby preventing the packaging products from environmental deterioration and flavor loss. Also, it could prevent small molecules from moving from the inside of the packaging to the outside, thereby protecting the product's shelf life.[11,12] Thus, designing a coating that balances environmental friendliness with high-barrier properties could improve the overall performance of paper-based packaging.

Montmorillonite (MMT) is a layered silicate mineral that belongs to the class of inorganic nanoparticles; it is an ultrafine particle with dimensions of a length between 1–100 nm in two or three dimensions.[13,14] Since it is a natural resource with abundant sources, it has been widely used for the following reasons:[15,16] Firstly, the MMT is easy to absorb water and dissolve, and possesses a large swelling property.[17] Therefore, the distance between the layers of MMT crystals increases, thereby promoting the reaction. Secondly, MMT belongs to the lamellar 2 : 1 structure; its unit cell is constructed by interspersing two SiO_2 tetrahedra with one Al–O octahedron, and the cations between layers can be replaced. The original cations between layers can be exchanged for inorganic or organometallic cations,[18] thereby changing the surface polarity. In addition, MMT particles can be discretized as a layer-by-layer sheet with a diameter-to-thickness ratio exceeding 1000, resulting in a larger specific surface area and greater contact with more molecules or atoms. Moreover, the obvious economic advantage is brought by low cost. However, natural montmorillonite has poor compatibility with the polymer matrix due to the high concentration of metal ions between its layers. Organic modification technology can increase the interlayer spacing of montmorillonite and enhance its compatibility with polymers. Therefore, organic montmorillonite (OMMT) is applied.[19] Since the OMMT is a nanoscale layer, it is often incorporated between polymers and composited into a new type of polymer composites called polymer/layered silicate nanocomposites, which have the following advantages:[20] a small addition amount is needed to enhance the mechanical strength and barrier properties of the composites.[21]

Additionally, they are lightweight, inexpensive, and thermally stable. More prominently, the excellent mechanical properties of the nanocomposites are attributed to the fact that the fillers improve their mechanical strength in the two-dimensional direction. It can be seen that polymer/lamellar silicate nanocomposites can address some of the polymers' defects, thereby greatly improving their comprehensive performance and showing great potential to enhance the moisture barrier performance of packaging materials. Therefore, polymer/lamellar silicate nanocomposites have not only reclaimed a significant market share in industrial construction but also presented significant business opportunities in the packaging field, which has become a focus of research and development for current packaging materials. Nylon/montmorillonite has been a key driver of nanocomposite development, and it was also the first time the intercalation modification method was used in the synthesis of nanocomposites.[22,23] In recent years, many institutions have conducted in-depth investigations into the synthesis of nanocomposites using the intercalation composite method[24] and have successfully developed polymer/clay nanocomposites tailored to polymer needs. The polymers usually used include nylon VI, polyvinyl alcohol, poly(ethylene terephthalate), epoxy resins, poly(ethylene glycol), glycol ester, polyethylene, and polyethylene oxide.[25–27] From the perspective of structural properties and applications, OMMT, as a nanoparticle filler, can improve the mechanical properties of composites and has significant development potential through intercalation modification.

Polyvinyl alcohol (PVA) is an organic compound with a molecular structure containing multiple hydroxyl groups, which has the appearance of a white, flaky, flocculent, or powdery solid. According to the degree of alcoholysis, PVA has been divided into three types: high, medium, and low.[28] When PVA is dissolved in water, the higher the degree of alcoholysis and the higher the concentration of the solution, the more viscous the solution will be, which enhances its strength and solvent resistance.[29,30] Due to the presence of a large number of hydroxyl groups on the surface of PVA, it is highly absorbent and water-soluble.[31] At the same time, the small size and high crystallinity of the side groups of PVA make it difficult for gases to penetrate, so that its gas barrier properties remain good under low humidity.[32] PVA also has good film-forming properties and can be prepared into a film that has a high gloss, non-electrically charged surface, good mechanical properties, and heat sealing by PVA solution.[33–36] Therefore, many researchers used PVA as a coating solution on substrates. In the early times, the 8511 Research Institute in China conducted the first research and developed the 1st-generation PVA coating solution.[37] The 1st-generation of coating solution could only be applied to the coating of biaxially oriented polypropylene and polyethylene films. In addition, some researchers added inorganic nanoparticles into the PVA coating solution to endow it with high barrier properties. Polyethylene terephthalate/polyvinyl alcohol/cast polypropylene can be prepared as a composite-coated film with a good barrier to water vapor, exhibiting a tenfold increase in oxygen barrier compared to the same thickness of the polyvinylidene dichloride-coated film.[38,39] In short, PVA has become a key material in coating fluids due to its excellent film-forming and barrier properties. By compounding with inorganic nanoparticles, such as MMT or other polymers, PVA offers broad application prospects for high-barrier, environmentally friendly packaging. The applications of PVA coatings in packaging can be summarized as follows. On the one hand, zeolitic protein nanoparticles containing cinnamaldehyde were incorporated into PVA/chitosan films for fresh-keeping packaging of pomfret. It has been shown that PVA not only acts as a matrix for bioactive compounds but also contributes to the overall stability of the composite film.[40]

On the other hand, in the development of packaging materials, PVA/bentonite coating can produce a paper packaging material that is water and oil-resistant. This study showed that PVA can significantly enhance the functional properties of paper-based materials.[41] To improve the barrier properties of

packaging, PVA/chitosan composite coatings can enhance the barrier performance of coated paper used for the preservation of agricultural products. The results showed that the coated paper could be used as a packaging material for fruits and vegetables, reducing weight loss and exhibiting lower color differences and better sensory evaluation.[42] PVA coatings have a promising future in packaging materials. However, PVA coatings still present some issues; for example, they are prone to moisture absorption under humid conditions, which reduces their barrier properties. Meanwhile, due to PVA's surface activity, foam may be generated during stirring of the PVA coating solution and during application to the substrate; thus, it is necessary to add a defoamer to address this issue.

In this study, montmorillonite was used as a nanoparticle filler, which was first intercalated and surface-modified to improve its water resistance, yielding organic montmorillonite. Then OMMT was added to PVA *via* solution intercalation compounding, and PVA/OMMT composite coatings were finally prepared using sodium tetraborate as a crosslinking agent, glycerol as a plasticizer, and tributyl phosphate as a defoamer. Meanwhile, the composite coatings were applied to the surface of Kraft paper *via* a facile automated coating process to construct the high-barrier PVA/OMMT-coated paper. The coated Kraft paper was characterized for morphology, mechanical properties, and barrier performance to evaluate its practicality as a barrier coating. The results showed that a combination of appropriate amounts of organic montmorillonite and polyvinyl alcohol made the Kraft paper structure denser and effectively blocked the entry of small molecules. Therefore, it is highly necessary to conduct this research, which can provide the packaging industry with an efficient method for producing high-barrier coatings for sustainable packaging materials that meet current sustainable development requirements for green packaging.

Materials and methods

Materials

Calcium-based montmorillonite (85% purity) was obtained from Guzhang County Shanlin Shiyu Stone Language Minerals Co., Ltd. Octadecyl trimethyl ammonium chloride (A-18), polyvinyl alcohol (1799 type; molecular weight: 31 000), and 3-aminopropyltriethoxysilane (KH-550) were provided by Shanghai McLean Biochemical Technology Co., Ltd. Glycerol (GI) was purchased from Tianjin Fuyu Fine Chemical Co., Ltd. Kraft paper (made from the pulp fibers of Masson pine; basis weight: 40 g m^{-2}) was obtained from Shandong Chenming Paper Industry Group Co., Ltd. Tributyl phosphate (TBP) was supplied by Wuxi Yatai United Chemical Co., Ltd. Sodium tetraborate was purchased from Guangdong Reagent Technology Co., Ltd. All other chemicals were AR grade and could be used without further purification.

Synthesis of PVA/OMMT composite coating

3.135 g of MMT was mixed with 200 mL of deionized water. The mixture was stirred using ultrasonic dispersion for 0.5 h, and the MMT suspension was finally obtained. 2.088 g of octadecyl trimethyl ammonium chloride was mixed with 100 mL of deionized water and stirred for 0.5 h in an 80 °C electric-heated thermostatic water bath. Then the MMT suspension was added into the composite liquid and stirred in an 80 °C electric-heated thermostatic water bath for 6 h. Next, the mixture was cooled to room temperature and allowed to precipitate for 12 h. After the upper layer of the mixture was poured off, the residue was washed with deionized water and then centrifuged by a high-speed table-top centrifuge (5000 rpm/10 min), and this operation was repeated 5 times. Finally, the mixture was placed in the electric drying oven at 80 °C for 6 h. After being ground to 80 mesh, the pillar-bearing MMT was sealed and stored. By mixing and stirring the pillar-bearing MMT with deionized water, a 20% mass fraction solution was prepared. Next, 1.0% silane coupling agent KH-550 was added into the solution and stirred in a 40 °C electric-heated thermostatic water bath for 5 h. Finally, the solution was placed in the electric drying oven at 80 °C for 6 h. After being ground to 200 mesh, the modified organic montmorillonite (OMMT) was obtained and sealed.

The modified OMMT was mixed with 30 mL of deionized water and stirred using ultrasonic dispersion for 0.5 h. Then, 5 g PVA was mixed with 60 g deionized water and stirred at room temperature in a water bath. Next, the temperature was turned to 95 °C and stirred continually until the PVA was completely dissolved (viscosity: 6.43 mPa s). Then, the modified OMMT suspension was added to the mixture, along with 2.5 mL of glycerol and 0.75 mL of tributyl phosphate. After the reaction was complete, a small amount of sodium tetraborate was slowly added to the solution. The water bath temperature was adjusted to 80 °C with low-speed stirring for 1 h, then cooled to room temperature. Ultimately, the solution was held for 12 h, after which a PVA/OMMT composite coating solution was obtained.

PVA/OMMT coating applied onto food packaging base paper

The Kraft paper used as a food packaging base paper was placed on an automatic coating machine, and then coated with the composite coating prepared by 11 different experimental formulations (Table 1). Afterward, the coated paper was dried under natural air-drying conditions for 12 h before use.

Thickness test

The thickness meter was first placed on a flat desktop, and then the paper sample was placed horizontally between the two planes. Subsequently, the two active planes of the instrument were gently pressed on the paper sample. Five points were randomly selected for testing, and the relevant data were recorded to determine the average.

Dissolution rate testing of PVA/OMMT composite film

The dissolution rate S (%) of the film was tested by the mass gain method.[43] A certain mass of dry film was placed in 30 mL of ultrapure water for 5 min, and then removed. The excess water on the surface of the sample composite film was wiped dry with paper. The dissolution rate test was repeated three times for

Table 1 The configuration of PVA/OMMT composite coating solutions

Sample	PVA	Modified montmorillonite	Sodium tetraborate	Glycerol	Tributyl phosphate	Deionized water
1	5.0 g	0.0 g	0.0 g	2.5 mL	0.75 mL	100 mL
2	5.0 g	1.0 g	0.03 g	2.5 mL	0.75 mL	100 mL
3	5.0 g	1.0 g	0.04 g	2.5 mL	0.75 mL	100 mL
4	5.0 g	1.0 g	0.05 g	2.5 mL	0.75 mL	100 mL
5	5.0 g	1.0 g	0.06 g	2.5 mL	0.75 mL	100 mL
6	5.0 g	1.0 g	0.07 g	2.5 mL	0.75 mL	100 mL
7	5.0 g	0.0 g	0.07 g	2.5 mL	0.75 mL	100 mL
8	5.0 g	0.5 g	0.07 g	2.5 mL	0.75 mL	100 mL
9	5.0 g	1.5 g	0.07 g	2.5 mL	0.75 mL	100 mL
10	5.0 g	2.0 g	0.07 g	2.5 mL	0.75 mL	100 mL
11	5.0 g	3.0 g	0.07 g	2.5 mL	0.75 mL	100 mL

each composite film sample. The calculation formula is shown below:

$$S = \frac{(W_{wet} - W_{dry})}{W_{dry}} \times 100\% \quad (1)$$

where W_{dry} was the mass of the composite film before swelling, and W_{wet} was the mass of the composite film after absorbing water and swelling.

ATR-FTIR testing

The coated paper was tested using a Fourier transform infrared (FTIR) spectrometer. The test wavelength range was 500 cm^{-1} to 4000 cm^{-1}. Before the test, the paper sample was cut into small pieces according to the requirements, and then the coating surface of the paper was pressed tightly with a sampler. Finally, the composition effect of the coating solution on paper performance was analyzed using the data.

SEM analysis

Before the test, the coated paper sample was cut and then fixed on the sample stage. Then, to make the sample conductive, the coating surface was treated with gold spray, and the surface topography was photographed and analyzed using a scanning electron microscope (SEM) at an accelerating voltage of 10.0 kV and a working distance of 10.5 mm.

Mechanical property testing

The paper was cut into 100 mm-long, 10 mm-wide strips, and the paper sample was tensile-tested using a GBH-1 electronic universal testing machine. The test conditions were: 25 °C and 75% humidity, a gauge distance of 25 mm, and a test speed of 100 mm min^{-1}. The vertical strength of the coated paper for each sample set was tested, and the experiment was repeated 3 times. The tensile strength (TS) was calculated as follows:

$$TS = \frac{F}{S} \quad (2)$$

where F (N) and S (m^2) were the tensile force of the sample that was subjected to and the area of the sample, respectively, and TS (MPa) was the tensile strength. Elongation at break (Elongation) was calculated as follows:

$$E = \frac{(L - L_0)}{L_0} \times 100\% \quad (3)$$

where E (%) and L_0 (mm) were the elongation at break and the length of the coated paper sample, respectively. And L (mm) was the standard distance at which the coated paper sample breaks. The modulus of elasticity (E) was calculated as follows:

$$E = \frac{\sigma}{\varepsilon} \quad (4)$$

where E (MPa) and σ (N) were the modulus of elasticity and stress, respectively, and ε (%) was the strain.

The density was calculated based on the paper's basis weight and the thickness. Bendtsen porosity was determined using an air permeance tester (L&W166, Sweden) according to ISO 5636-3.

Oil contact angle testing

The oil contact angles of different papers were measured using a surface contact angle tester (OCA40, Dataphysics) to analyze their oil barrier properties. The test solution was castor oil, with a droplet volume of 5 μL. After the droplet was dropped, contact times were recorded at different times.

Oxygen permeability testing

The oxygen permeability (OP) of the paper samples was determined using the VAC-VI gas permeation meter (Labthink, China) at 23.0 ± 2.0 °C and 50 ± 5% humidity, according to the ISO 15105-1-2007 standard method. The sample permeation area was 50.0 cm^2, and the partial pressure gradient was 105.0 kPa. The OP was expressed with the unit of cm^3 m^{-2} 24 h Pa, and transmission rate (OTR) was expressed with the unit of cm^3 cm cm^{-2} s Pa. Each sample was measured in triplicate.

Water vapor permeability testing

The water vapor permeability (WVP) measurements were performed by a laboratory-designed testing system according to the previous method.[44] The WVP value was calculated by measuring the weight change of moisture passing through the sample per

unit time, the unit was g cm cm^{-2} s Pa. Each sample was measured in triplicate.

Results and discussion

In this study, PVA was used as the film-forming substrate, and modified organic montmorillonite as the filler. At the same time, a certain amount of plasticizer (glycerol), defoamer (tributyl phosphate), and crosslinking agent (sodium tetraborate) was added to form the PVA/OMMT composite coating solution *via* solution intercalation. Then, it was evenly coated onto the surface of Kraft paper using an automatic coating machine. After drying, a coating layer formed, resulting in a high-barrier coating liquid and endowing the Kraft paper with excellent barrier properties. The schematic diagram of the PVA/OMMT coating and coated paper preparation process is exhibited in Fig. 1. The PVA/OMMT coating solution was prepared by setting sodium tetraborate and montmorillonite as univariate variables, and other ingredients as invariants. As shown in Table 1, sample 1 was the control pure PVA coating solution for the various experimental groups. Samples 2–6 were the amounts (0.03 g, 0.04 g, 0.05 g, 0.06 g, 0.07 g) of sodium tetraborate added when the modified organic montmorillonite addition was 1.0 g; Samples 6–11 were the amounts (1.0 g, 0 g, 0.5 g, 1.5 g, 2.0 g, 3.0 g) of montmorillonite added when the amount of sodium tetraborate added was 0.07 g, respectively. Sample 0 represented the original kraft paper.

The coating solution prepared by the above 11 experimental groups was coated on the Kraft paper, and the thickness of the Kraft paper coated by different experimental schemes is shown in Table 2. The original Kraft paper was 0.132 mm thick. According to the data, the Kraft paper coated with the coating solution, which contained unmodified montmorillonite and sodium tetraborate, had the lowest thickness, and the thickness increased significantly after coating, indicating that the coating solution could effectively increase the Kraft paper thickness. However, with increasing OMMT (sodium tetraborate), the thickness of the coated paper did not increase proportionally, indicating that the coating solutions prepared under different experimental schemes had different effects on the thickness of the coated Kraft paper. In addition, the basis weight of different coated papers was positively correlated with their thickness, with values generally falling within the range of 45–46 g m^{-2}. During the coating process, part of the coating solution entered the internal network of the Kraft paper, while the rest adhered to its surface. In short, these data could provide an important reference for optimizing the Kraft paper coating process.

Fig. 2a showed the swelling ratio of the composite coating prepared by pure PVA coating solution and single variable sodium tetraborate addition. The single variable sodium tetraborate was 0.03 g, 0.04 g, 0.05 g, 0.06 g, 0.07 g, and the amount of OMMT was kept unchanged at 1.0 g. The diagram shows that the adsorption force of water molecules on the composite film decreased gradually with increasing sodium tetraborate amount. The highest decreased from 108.08% to 45.76%. Since the PVA can be dissolved in water and the surface of PVA modified by sodium tetraborate containing a large amount of –OH, the adsorption capacity of water molecules was stronger. In addition, a crosslinking reaction occurred in PVA modified with sodium tetraborate, thereby enhancing the composite film's water resistance. In this case, the optimal amount of sodium tetraborate was 0.07 g. Fig. 2b showed the effect of the composite coating film made with the pure PVA coating solution and a single-variable OMMT addition on the swelling ratio. The single-variable OMMT was 0.5 g, 1.0 g, 1.5 g, 2.0 g, and 3.0 g, and the amount of sodium tetraborate to add was kept constant

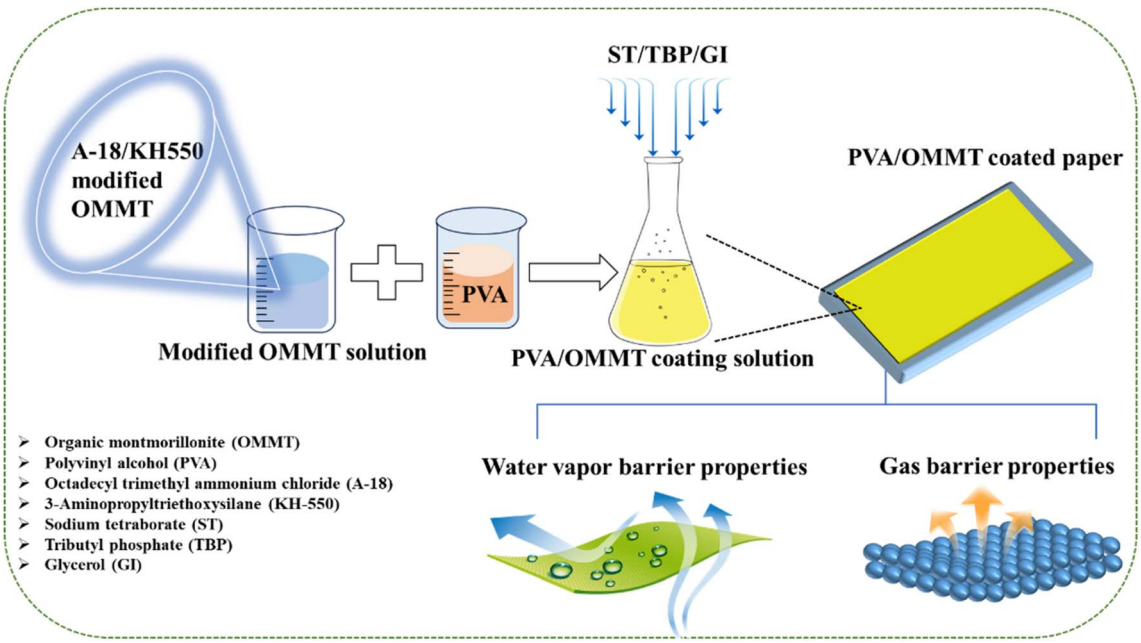

Fig. 1 A schematic diagram of the PVA/OMMT composite coating and coated paper preparation process.

Table 2 Thicknesses of various PVA/OMMT-coated paper samples

Sample	Thicknesses (mm)					Average value (mm)	Basis weight (g m^{-2})
0	0.136	0.130	0.134	0.129	0.131	0.132	40.000
1	0.155	0.151	0.154	0.152	0.153	0.153	45.242
2	0.160	0.159	0.161	0.159	0.158	0.159	45.301
3	0.162	0.163	0.163	0.162	0.165	0.163	45.394
4	0.164	0.168	0.166	0.167	0.165	0.166	45.473
5	0.167	0.168	0.165	0.169	0.166	0.167	45.526
6	0.166	0.170	0.169	0.169	0.166	0.168	45.681
7	0.160	0.163	0.162	0.163	0.161	0.162	45.439
8	0.166	0.164	0.165	0.166	0.164	0.165	45.505
9	0.168	0.170	0.172	0.167	0.168	0.169	45.698
10	0.170	0.173	0.172	0.169	0.171	0.171	45.727
11	0.173	0.170	0.171	0.173	0.173	0.172	45.745

at 0.07 g. It can be seen that, with increasing OMMT, the films' swelling ratio decreased initially and then increased, and the optimal OMMT addition was 1.0 g. Adding an appropriate amount of OMMT can be combined with PVA to make the structure dense and block the entry of water molecules. At the same time, OMMT was a powder that easily adsorbed water molecules, so that excessive OMMT would increase the adsorption capacity of water molecules, and the swelling ratio would increase. The appearance of the coating solution is also shown. Fig. 2c shows the low viscosity of the PVA/OMMT composite coating (viscosity: 4.72 mPa s), and Fig. 2d shows the high viscosity of the PVA/OMMT composite coating (viscosity: 33.86 mPa s). It was found that as the amount of sodium tetraborate increased, the viscosity of the composite coating solution increased. However, as the sodium tetraborate content increased, the composite coating solution lost its flow-following property and became very viscous, making it impossible to coat.

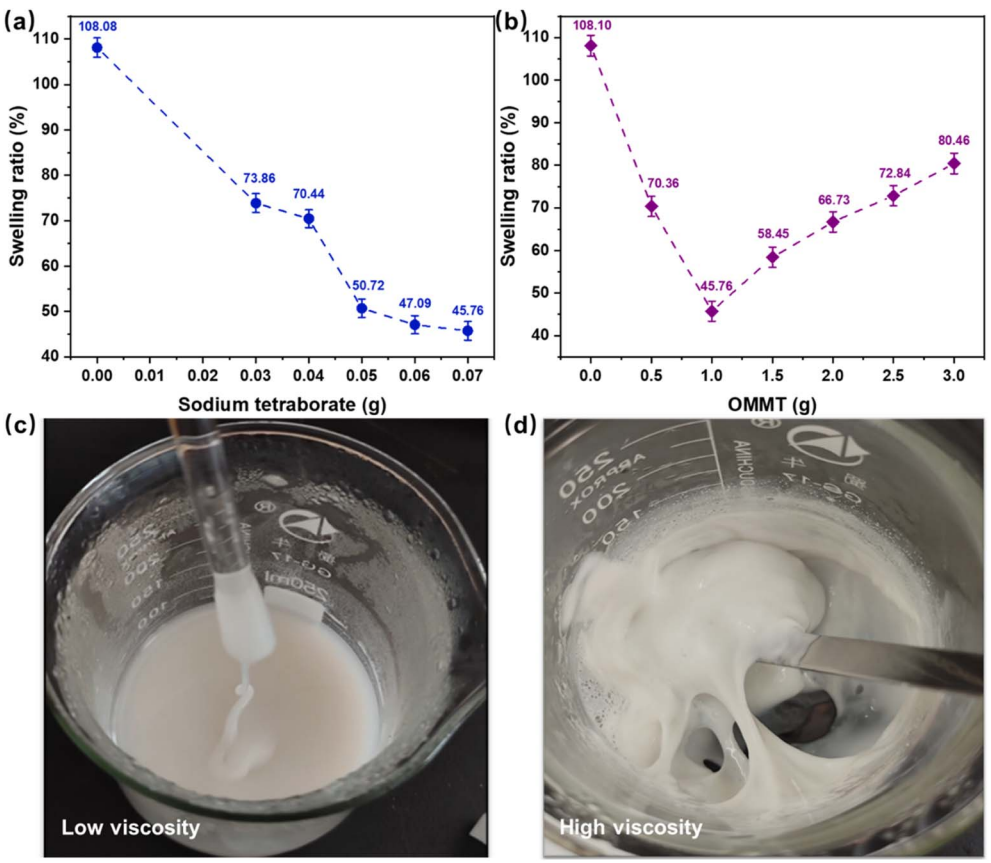

Fig. 2 (a) Effect of sodium tetraborate addition on the swelling ratio of the composite film. (b) Effect of OMMT addition on the swelling ratio of the composite film. Photographs of (c) low-viscosity PVA/OMMT composite coating and (d) high-viscosity PVA/OMMT composite coating.

Fig. 3a shows that montmorillonite has a layered structure composed of tetrahedral and octahedral sheets, with exchangeable cations. Fig. 3b shows the change in interlayer spacing of modified montmorillonite, indicating that octadecyl trimethyl ammonium chloride successfully entered the interlayer *via* a cation–exchange reaction, thereby increasing the interlayer spacing. The infrared spectrum analysis of Fig. 3c further verified the modification effect. The C–H symmetric stretching vibration peak appeared at 2920 cm^{-1}, the C–H antisymmetric stretching vibration peak appeared at 2848 cm^{-1}, and the ammonium salt absorption peak appeared at 1471 cm^{-1}. The appearance of these characteristic peaks indicated that octadecyl trimethyl ammonium chloride had successfully entered the layered structure of OMMT and realized interlayer cation exchange.[45–47]

Meanwhile, the hydroxyl vibration absorption peak intensity of the column-modified montmorillonite at 3440 cm^{-1} and 1648 cm^{-1} was significantly weaker than that of the unmodified montmorillonite, which indicated that the organic modification led to the weakening of –OH bonding and the decrease of hydrophilicity, which further confirmed that octadecyl trimethyl ammonium chloride entered the middle layer of OMMT. From the SEM image results, the aggregates of unmodified montmorillonite (Fig. 3d) showed a regular morphology, no curling, and clear crystallization. The pillar-supported modified montmorillonite (Fig. 3e) showed a loose structure with agglomerates and curls. The change in microstructure was consistent with the results of increased interlayer spacing, chemical bond changes, and organic modification, as reflected in Fig. 3a–c. Due to the insertion of organic matter, the interlayer spacing of the modified montmorillonite increased, and the structure became relatively loose. This was manifested in the SEM image as a change in the aggregates' morphology, in stark contrast to the regular morphology of unmodified montmorillonite. In summary, based on the overall analysis from the schematic diagram of the basic structure of montmorillonite, the change of interlayer spacing after modification, the modification effect by infrared spectroscopy, and the significant differences in the microstructure of montmorillonite before and after modification. They completely presented the structural characteristics of montmorillonite and the effect of the modification process on its structure and properties.

Moreover, the surfaces of the Kraft paper before and after coating were further investigated using SEM. The image in Fig. 4 clearly shows the surface morphology of the original Kraft paper, PVA-coated paper, and PVA/OMMT-coated paper (containing sodium tetraborate) at different magnifications. Fig. 4a and b was an electron microscope scan with 500× and 200× magnification of the surface of uncoated Kraft paper. The surface fibers of the uncoated Kraft paper were interlaced, and numerous pores were observed. These pores were the main channels for the penetration of small molecules, resulting in poor barrier properties. Fig. 4c and d was an electron microscope scan with 500× and 200× magnification of the surface of coated PVA Kraft paper. It can be seen that the number of surface fibers on Kraft paper coated with PVA was significantly reduced, and the pores were also smaller. Fig. 4e and f was an electron microscope scan with 500× and 200× magnification of

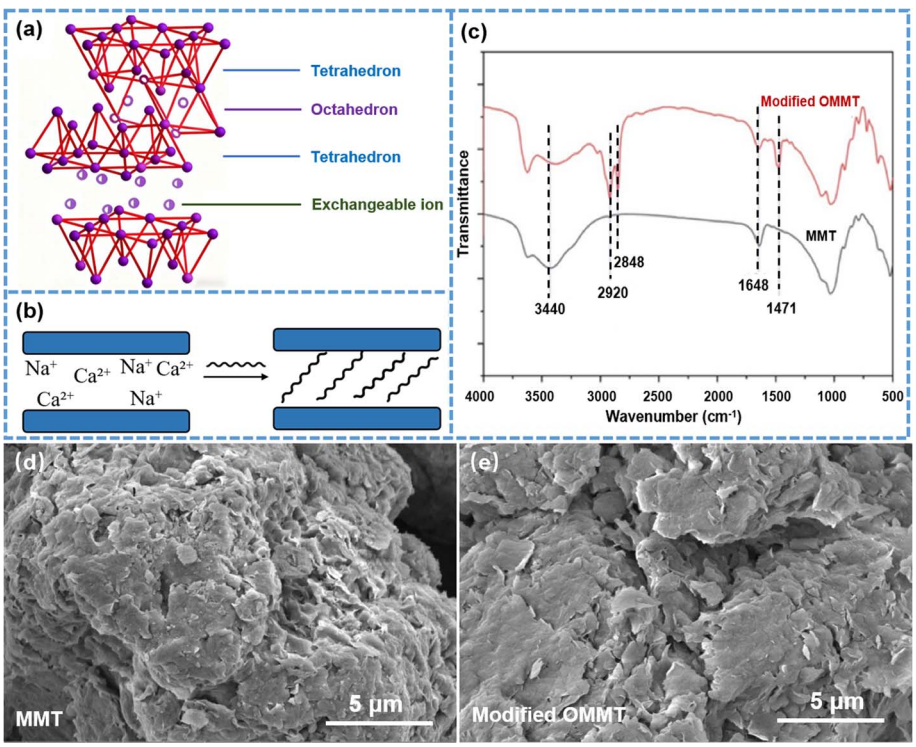

Fig. 3 (a) The structure of MMT. (b) Changes in the spacing of modified montmorillonite layers. (c) Infrared spectra of MMT before and after modification. Images showing the morphology of (d) MMT and (e) modified OMMT.

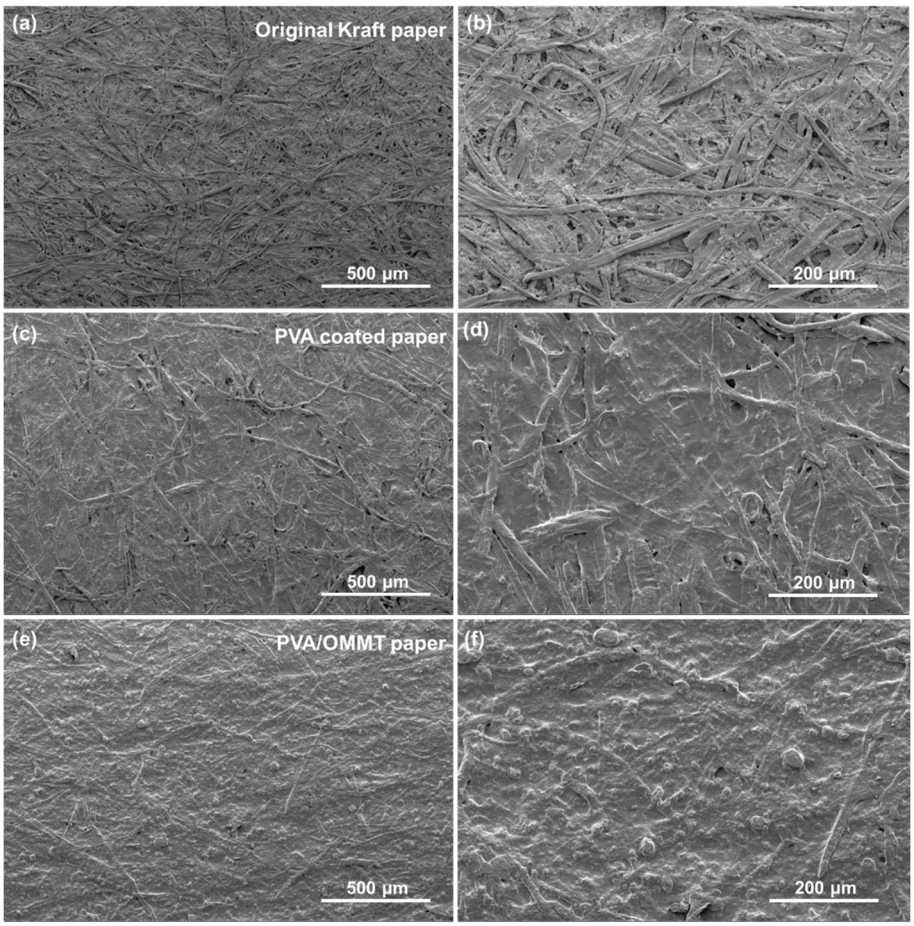

Fig. 4 Surface characteristics of different coated papers with various coatings: SEM images of (a and b) original Kraft paper, (c and d) PVA-coated paper, and (e and f) PVA/OMMT-coated paper.

the surface of coated PVA/OMMT Kraft paper. We found that after adding OMMT, the paper's surface morphology became more compact and complete, with pores almost disappearing. Due to the fine particles of montmorillonite in the PVA/OMMT coating solution filling the pores, and the crosslinking effect of sodium tetraborate, a dense network structure was further formed. This structure effectively blocked the penetration of small molecules, significantly improving the barrier properties of the coated paper. In general, due to crosslinking reactions between PVA and fillers such as OMMT or sodium tetraborate, the compactness and integrity of the paper surface gradually improved, and the barrier properties were also enhanced.

After tensile testing of coated paper with different sodium tetraborate contents, a line chart of mechanical properties, as shown in Fig. 5, was obtained. When the content of sodium tetraborate was 0.05 g, the tensile strength of PVA/OMMT-coated paper was the highest (23.05 MPa), and it was higher than that of coated paper without sodium tetraborate. Above 0.05 g, the tensile strength gradually decreased with the increase of sodium tetraborate content (Fig. 5a). When the content of sodium tetraborate in PVA/OMMT coated paper was 0.05 g, the coated paper can withstand the maximum force, which was due to the appropriate amount of sodium tetraborate could optimize the coating structure, promote crosslinking, make the Kraft paper fiber more closely, to improve the tensile strength of the coated paper. When the content of sodium tetraborate increased, the elastic modulus also increased, and it was higher than that of coated paper without sodium tetraborate. When the content of sodium tetraborate was 0.05 g, the elastic modulus of coated paper could reach 1961.35 MPa (Fig. 5b). When the content of sodium tetraborate in PVA/OMMT-coated paper was 0.05 g, the coated paper had the greatest ability to resist elastic deformation. This was due to the crosslinking reaction between sodium tetraborate and the hydroxyl group on the PVA molecular chain, forming a borate ester bond that restricted the movement of the PVA molecular chain segment, making the coating structure more compact and rigid and thereby increasing the elastic modulus of the coated paper. At the same time, the addition of sodium tetraborate optimized the interaction between PVA and OMMT, thereby enhancing interfacial bonding, improving stress transfer efficiency, and ultimately increasing the rigidity of the composite paper. In addition to affecting the force between PVA and OMMT, the coating on the surface of the paper also had an influence on the elongation at break. As shown in Fig. 5c, the elongation at break gradually decreased with increasing sodium

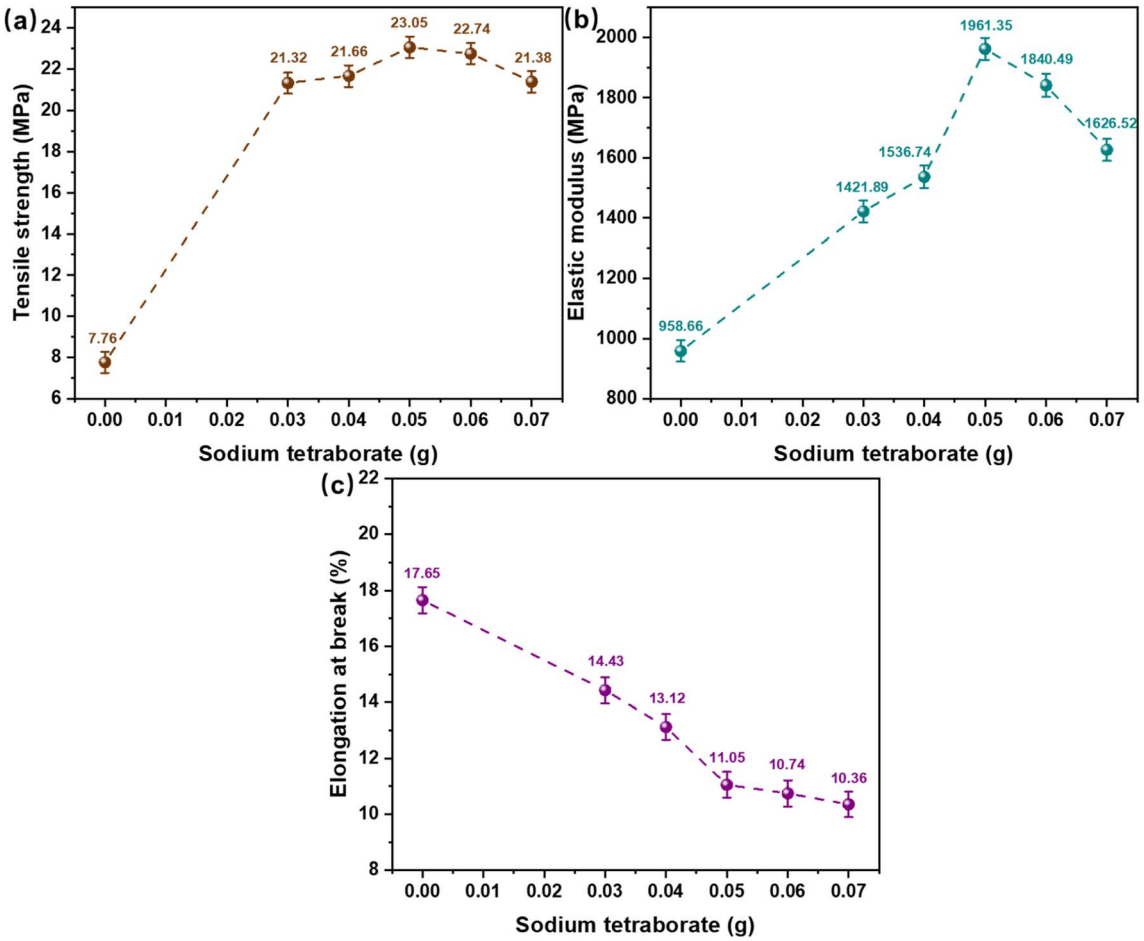

Fig. 5 Mechanical properties of coated paper with different sodium tetraborate content levels: (a) tensile strength, (b) elastic modulus, and (c) elongation at break.

tetraborate content, and all elongations at break after adding sodium tetraborate were lower than those without it. This was because the crosslinking effect from the addition of sodium tetraborate would limit the movement and sliding of the PVA molecular chains, making it difficult for them to stretch freely under external force, thereby decreasing the composite paper's elongation at break. Therefore, we found that, by balancing tensile strength and elastic modulus and accounting for a certain elongation at break, the optimal addition amount of sodium tetraborate in PVA/OMMT-coated paper was 0.05 g, and the mechanical properties of coated paper were the best.

After the tensile test of coated paper with different OMMT content, the mechanical performance line chart was obtained as shown in Fig. 6. When the OMMT content was 1.0 g, the tensile strength of PVA/OMMT-coated paper was the highest (30.27 MPa) and higher than that of the coated paper without OMMT. Above 1.0 g, the tensile strength gradually decreased with the increase of OMMT content (Fig. 6a). When the content of OMMT in PVA/OMMT-coated paper was 1.0 g, the coated paper could withstand the maximum force. This was because the OMMT surface typically contained active groups that could form hydrogen bonds with the PVA hydroxyl groups. The formation of hydrogen bonds strengthened the binding force between OMMT and PVA, thereby enhancing the intermolecular force of the entire coated paper. As OMMT content increased, the elastic modulus also increased and was higher than that of the coated paper without OMMT. When the OMMT content was 1.0 g, the elastic modulus of the coated paper was also the largest, with a value of 2647.41 MPa (Fig. 6b). When the content of OMMT in PVA/OMMT-coated paper was 1.0 g, the coated paper had the greatest ability to resist elastic deformation. Crosslinking between the active groups on the OMMT surface and the PVA molecular chains could enhance the composite paper's network structure. The crosslinking effect limited molecular chains' sliding and increased the elastic modulus when the paper was subjected to external forces.[12] As shown in Fig. 6c, the elongation at break initially increased and then decreased with increasing OMMT content. When the OMMT content was 1.0 g, the elongation at break was the largest of 12.23%. When the OMMT content was appropriate, the interaction between the PVA molecular chain and OMMT could impart the paper with a certain degree of strength during stretching, allowing a certain degree of deformation and thereby improving elongation at break. However, excessive OMMT would lead to ultra-crosslinking, increasing the composite paper's brittleness and reducing its elongation at

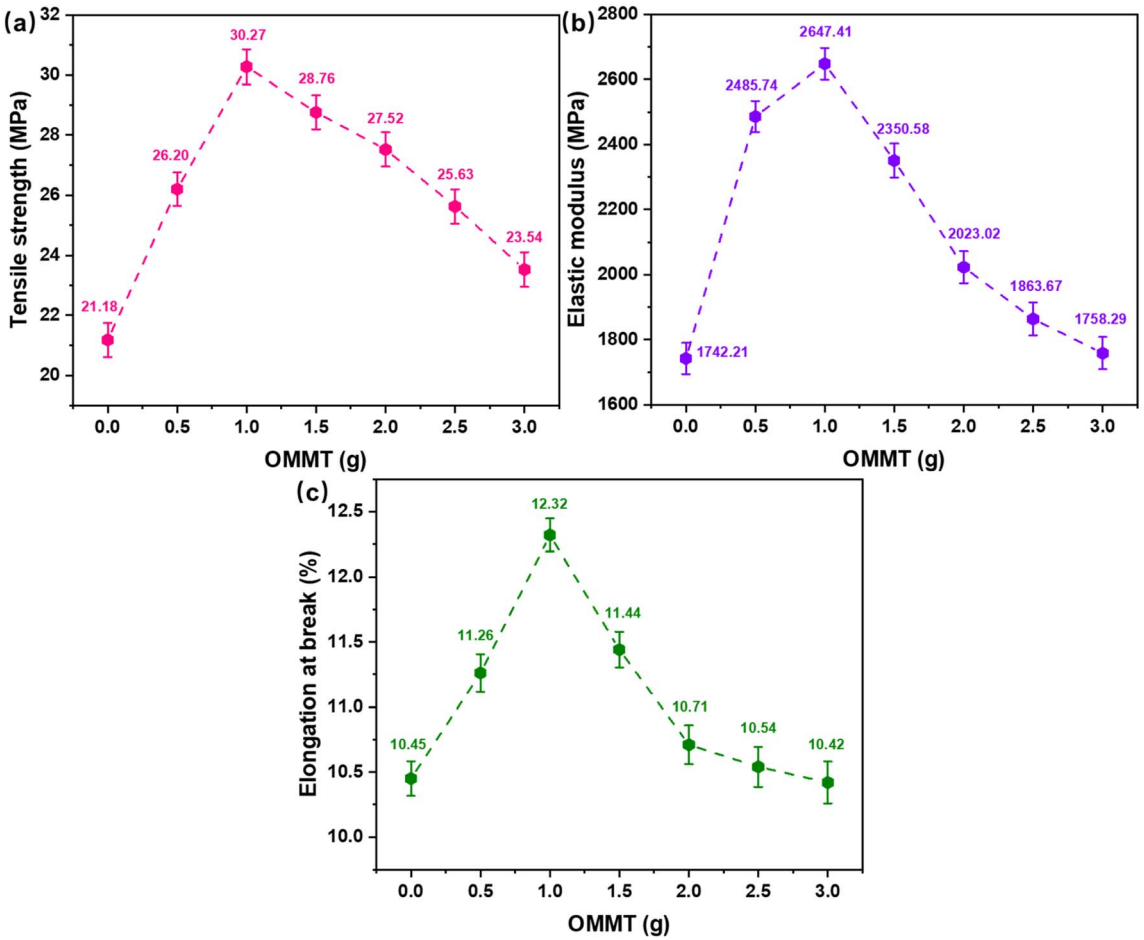

Fig. 6 Mechanical properties of coated paper with different OMMT content levels: (a) tensile strength, (b) elastic modulus, and (c) elongation at break.

break. Therefore, we found that, by balancing tensile strength and elastic modulus and accounting for a certain elongation at break, the optimal addition amount of OMMT in PVA/OMMT-coated paper was 1.0 g, and the coated paper exhibited the best mechanical properties under this condition.

Fig. 7a and b shows the oxygen permeability and oxygen transmission coefficient of PVA/OMMT-coated paper with different OMMT contents. As OMMT content increased, the oxygen permeability and oxygen transmission rate of the PVA/OMMT-coated paper gradually decreased. During the experiment, when the OMMT content was 3.0 g, the oxygen permeability and oxygen transmission rate of the PVA/OMMT/-coated paper were the lowest. The oxygen permeability of PVA/OMMT-coated paper decreased from 33.60 $cm^3\ m^{-2}\cdot 24$ h Pa to 14.92 $cm^3\ m^{-2}\cdot 24$ h Pa, and the oxygen transmission rate decreased from 3.89×10^{-11} cm^3 cm $cm^{-2}\ s^{-1}$ Pa to 1.72×10^{-11} cm^3 cm $cm^{-2}\ s^{-1}$ Pa when the OMMT content was 1.0 to 3.0 g. When OMMT is 0 to 1.5 g, oxygen permeability and oxygen transmission rate change significantly. After more than 1.5 g, the decline was more moderate. However, compared with the blank group (original Kraft paper), the oxygen permeability and oxygen transmission rate of Kraft paper treated with PVA/OMMT composite coating solution decreased significantly. Due to the combination of OMMT and PVA, OMMT was well dispersed within PVA, and a relatively close network structure was formed between them, creating a physical barrier within the composite paper, such as a labyrinthine path, which increased path length and tortuosity of oxygen transmission, greatly reducing oxygen penetration and lowering the oxygen penetration rate, thus providing excellent barrier performance. The oxygen penetration and diffusion paths of the composite coating-coated paper are shown in Fig. 7d. The effect of sodium tetraborate content on oxygen permeability is shown in Fig. 7c; it was found that sodium tetraborate content had little effect on the oxygen barrier. The oxygen permeability of PVA/OMMT-coated paper decreased from 27.21 $cm^3\ m^{-2}\cdot 24$ h Pa to 23.98 $cm^3\ m^{-2}\cdot 24$ h Pa as the amount of sodium tetraborate increased to 0.07 g. The addition of sodium tetraborate was mainly to enhance the water resistance of composite coatings in humid environments. However, it had little effect on the gas barrier properties of the composite coatings and could retain their gas barrier properties.

Fig. 8a showed the effect of different sodium tetraborate contents on the water vapor transmission rate (WVP) of coated paper. With the increase in sodium tetraborate content from 0.03 g to 0.07 g, the WVP showed an overall decreasing trend,

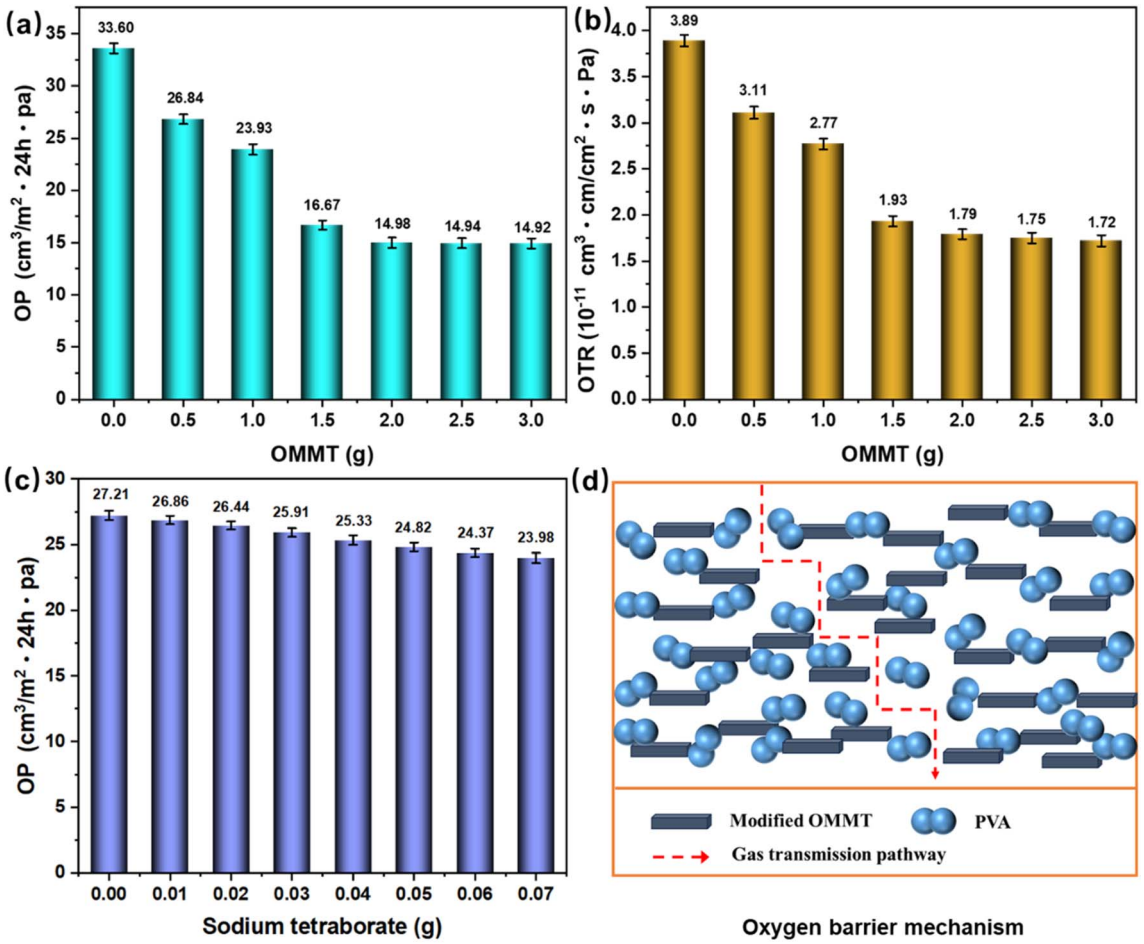

Fig. 7 (a) Oxygen permeability of coated paper with different OMMT content levels, (b) oxygen transmission rate of coated paper with different OMMT content levels, (c) oxygen permeability of coated paper with different sodium tetraborate content levels, and (d) an idealized model of the gas molecule transmission path provided by composite coatings.

but the rate of decrease gradually slowed. At the sodium tetraborate content of 0.07 g, the WVP reached the lowest value of 2.71×10^{-12} g cm cm^{-2} s^{-1} Pa. This was because sodium tetraborate could improve the water resistance of the coating solution, and when it crosslinked with PVA, the structure of the coated paper became more compact, hindering the transmission of water vapor molecules and reducing the moisture permeability coefficient of the coated paper. However, if too much sodium tetraborate was added, the viscosity of the composite coating solution was too high, which may lead to coating difficulties and affect the quality of the coated paper, and, in turn, have a certain negative impact on moisture permeability. Fig. 8b demonstrated the effect of different OMMT contents on the water vapor transmission rate of coated paper. As the OMMT content increased from 0.5 g to 3.0 g, the WVP first decreased and then increased, and then reached a minimum value of 2.68×10^{-12} g cm cm^{-2} s^{-1} Pa at the OMMT content of 1.0 g. This was because a moderate amount of OMMT can fill the pores of the coated paper, increasing its density, and thus, reducing the moisture vapor transmission coefficient. However, when the OMMT content was excessive, it may lead to an uneven internal structure of the coated paper and agglomeration, which in turn increases the channel for water vapor to pass through the coated paper and the moisture permeability coefficient. The study results showed that the addition of both sodium tetraborate and OMMT could affect the moisture permeability coefficient of the coated paper, and the primary reason was that these additives changed the structural densification of the coated paper. The barrier mechanism was revealed in Fig. 8c. The penetration of water vapor molecules from the high-concentration side to the low-concentration side required four steps: adsorption, dissolution, diffusion, and desorption.[48] The barrier properties of a material then depend on how well it impedes these steps. When the structure of the coated paper was dense and homogeneous, the diffusion path of water vapor molecules in the material became longer, and the diffusion difficulty increased, thus reducing the moisture permeability coefficient. Therefore, both the crosslinking reaction of sodium tetraborate and the filling effect of OMMT impeded the transmission of water vapor by making the structure of the coated paper denser and increasing the curvature and length of the diffusion path of water vapor molecules.

Additionally, the effect of the sodium tetraborate and OMMT on oil barriers was also investigated, and the results were

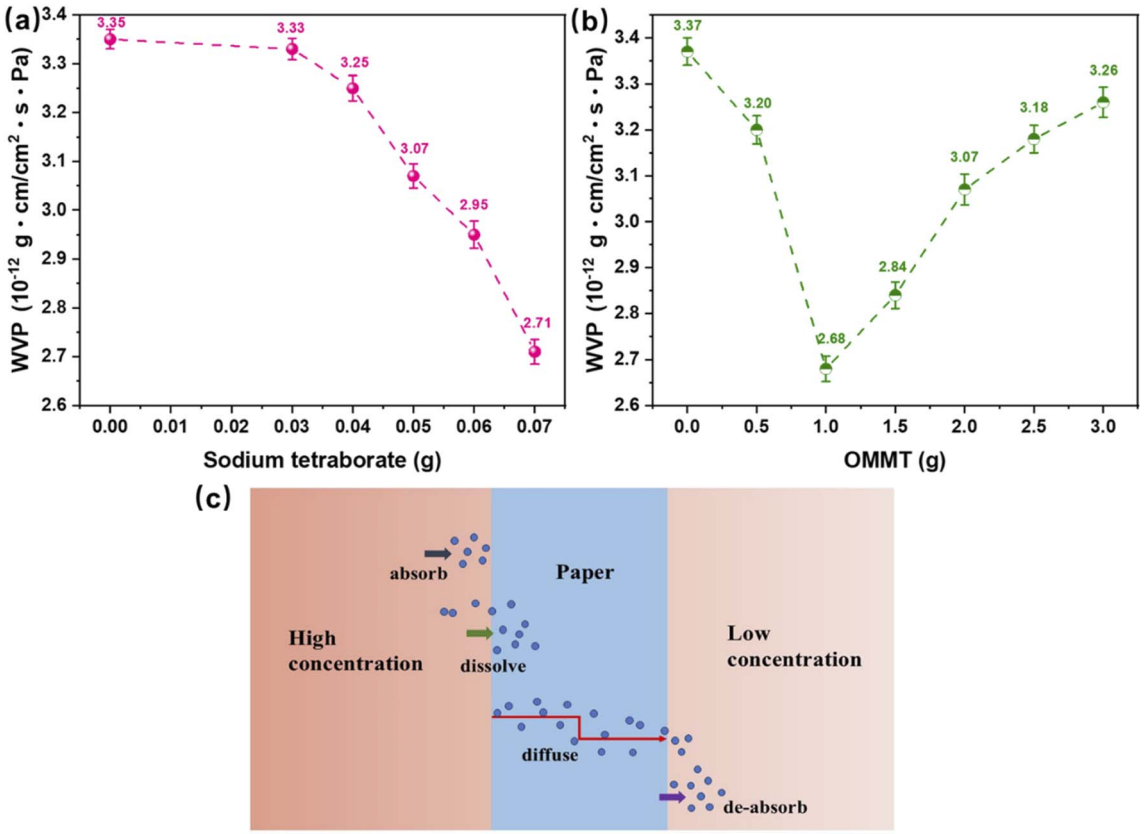

Fig. 8 (a) Water vapor transmission rate of coated paper with different sodium tetraborate content levels. (b) Water vapor transmission rate of coated paper with different OMMT content levels. (c) A diagram of the water vapor molecule barrier mechanism.

presented in Table 3. The initial oil contact angles of all samples were less than 90°, indicating that the composite coating did not impart an oil-repellent effect on the paper. However, with the extension of the contact time of oil droplets (0–2 min), the oil contact angle of the original Kraft paper rapidly decreased from 41.37° to 13.64°. This was mainly because the penetration of oil droplets into the Kraft paper accelerated their spread on the base paper. With the extension of the oil droplet contact time (0–2 min), the rate at which the oil contact angle of the composite coated paper decreases gradually, and the contact angle finally stabilizes basically within the range of 15–18°. This was because the barrier effect of the composite coating made the oil droplets only spread on the surface of the paper and did not penetrate into the base paper. The result indicated that although the composite coating cannot reduce the critical surface tension of Kraft paper, it had a certain oil resistance, enhancing the barrier effect on the Kraft paper.

Table 3 Oil droplet contact angle changes with time

	Oil droplet contact angle (°)					
Sample	0 min	2 min	4 min	6 min	8 min	10 min
0	41.37	13.64	13.02	12.15	11.83	11.37
1	41.45	32.81	26.87	21.93	17.88	15.02
2	42.13	33.62	27.74	22.54	18.43	15.59
3	42.87	34.47	28.56	23.12	18.85	16.18
4	43.01	34.86	28.91	23.58	19.17	16.46
5	43.26	35.24	29.17	23.92	19.64	16.67
6	43.52	35.68	29.54	24.16	19.85	16.84
7	42.75	34.93	28.85	23.54	19.05	16.12
8	43.16	35.27	29.10	23.82	19.40	16.51
9	43.83	35.96	29.87	24.50	20.18	17.01
10	44.20	36.41	30.16	24.88	20.53	17.37
11	44.57	36.82	30.51	25.12	20.89	17.54

Conclusions

In this work, montmorillonite was first modified by octadecyl trimethyl ammonium chloride for column support, and the silane coupling agent 3-amino-propyltriethoxysilane was utilized for surface modification to obtain organic montmorillonite. OMMT was then mixed with polyvinyl alcohol to prepare the functional PVA/OMMT composite coatings, which were finally coated onto Kraft paper. The effects of different sodium tetraborate and OMMT levels on the barrier and mechanical properties of PVA/OMMT-coated paper were investigated by the univariate method. It is worth noting that the barrier properties of PVA/OMMT-coated paper were significantly improved by the synergistic effect of the composite coating and the Kraft paper matrix. The oxygen permeability of PVA/OMMT-coated paper was reduced to 14.92 $cm^3\ m^{-2}\cdot 24\ h\ Pa$, and the water vapor transmission rate was reduced to 2.68×10^{-12} g cm $cm^{-2}\ s^{-1}$

Pa. This was attributed to the crosslinking of OMMT with PVA, which could improve the dense structure of the coated paper, thereby enhancing its barrier properties. Moreover, the coated paper had a certain oil resistance effect by enhancing the barrier effect on the Kraft paper. The study suggested that a PVA/OMMT composite coating could be successfully applied to Kraft paper to produce coated paper with excellent barrier and mechanical properties, thereby improving the overall quality of paper-based packaging materials and being of great significance in the development of the green packaging field.

Ethical statement

This article does not contain any studies with human participants or animals performed by any of the authors.

Author contributions

Zheng Cheng: Supervision, visualization, writing-review & editing. Mei Ning: Writing-original draft, investigation. Xinmei Nong: Methodology, visualization. Naiyu Xiao: Methodology, project administration. Xueqin Zhang: Conceptualization, data curation. Le Zhong: Methodology, formal analysis. Honglei Wang: Resources, writing-review & editing. Guojian Chen: Validation, methodology. Qianbin Mo: Investigation, formal analysis.

Conflicts of interest

The authors declare no conflicts of interest.

Data availability

All data and materials are available on request. Correspondence and requests for materials and data should be addressed to Zheng Cheng.

Acknowledgements

The research is supported by the Science and Technology Planning Project of Guangzhou (2024A04J2301 & 2024E04J1231 & 2023B01J2001), the Fundamental Research Funds from the Zhongkai University of Agriculture and Engineering (KA25YY17011), and the State Key Laboratory of Advanced Papermaking and Paper-based Materials (202501). We are grateful for this financial support.

References

1 M. Rabnawaz, I. Wyman, R. Auras and S. Cheng, *Green Chem.*, 2017, **19**, 4737–4753.
2 S. Zhao, Y. Zha, X. Guo and T.-M. Choi, *Int. J. Prod. Res.*, 2025, 1–20.
3 H. Jia-ling, Z. Tian-long, C. Jie, L. Qin-bao, Z. Huai-ning and M. Jing-li, *J. Instrum. Anal.*, 2021, **40**, 1672–1680.
4 Z. Cheng, J. Li, M. Su, N. Xiao, L. Zhong, X. Zhang, M. Liu, Q. Chen and J. Zhou, *RSC Adv.*, 2024, **14**, 20479–20491.
5 H. Srinivasan, H. Arumugam, A. Ami and A. Muthukaruppan, *Cellulose*, 2024, **31**, 7713–7725.
6 P. Kumar, A. Kishore, S. Tripathi, Lavanya, V. Chaudhary and K. K. Gaikwad, *Biomass Convers. Biorefin.*, 2025, **15**, 13037–13053.
7 L. Li, Y. Wang, T. Lei, Z. Xie and Y. Liang, *J. Porous Mater.*, 2024, **31**, 887–895.
8 S. Basak, M. S. Dangate and S. Samy, *Prog. Org. Coat.*, 2024, **186**, 107938.
9 X. Du, L. Hou, Y. Cheng, L. Chen, X. Chen, L. Mo, G. Yu, H. Li, X. Zhang and H. Zhang, *Cellulose*, 2024, **31**, 11131–11145.
10 P. K. Kunam, D. Ramakanth, K. Akhila and K. K. Gaikwad, *Biomass Convers. Biorefin.*, 2024, **14**, 12637–12652.
11 E. Pasquier, B. D. Mattos, H. Koivula, A. Khakalo, M. N. Belgacem, O. J. Rojas and J. Bras, *ACS Appl. Mater. Interfaces*, 2022, **14**, 30236–30245.
12 Z. Cheng, J. Li, M. Su, N. Xiao, L. Zhong, X. Zhang, S. Chen, Q. Chen, W. Liang and M. Liu, *ACS Appl. Polym. Mater.*, 2024, **6**, 2877–2888.
13 B. Şengül, R. M. A. El-abassy, A. Materny and N. Dilsiz, *Polym. Sci., Ser. A*, 2017, **59**, 891–901.
14 Y. Chang, K. Guo, L. Guo, X. Liu, G. Chen, H. Liu, H. Yang and J. Chen, *J. Electrost.*, 2016, **80**, 17–21.
15 J. Ding, L. Liao, P. Shuai, Q. Guo and L. Mei, *Inorg. Chem.*, 2023, **62**, 19070–19079.
16 X. Xiang, N. Shen, X. Wang, L. Su, L. Xu and F. Wu, *Polym. Eng. Sci.*, 2022, **62**, 687–693.
17 M. Zemzem, L. Vinches and S. Hallé, *J. Elastomers Plast.*, 2021, **53**, 009524432110061.
18 B. Nunes, F. Cagide, C. Fernandes, A. Borges, F. Borges and M. Simões, *Int. J. Mol. Sci.*, 2024, 25.
19 L. Yan, Z. Xu and X. Wang, *Prog. Org. Coat.*, 2018, **122**, 107–118.
20 G. Kumaraswamy, Y. Deshmukh, V. V. Agrawal and P. Rajmohanan, *J. Phys. Chem. B*, 2005, **109**, 16034–16039.
21 M. Dabbaghianamiri, E.-s. M. Duraia and G. W. Beall, *Results Mater.*, 2020, **7**, 100101.
22 Q. Yang, Z. Yang, F. Lu, H. Ge, Y. Du, D. Cao, Z. Yuan and C. Lu, *Anal. Chem.*, 2024, **96**, 4657–4664.
23 F. Liu, Y. Zhang, X. Xiao, Y. Cao, W. Jiao, H. Bai, L. Yu and Q. Duan, *Chem. Eng. J.*, 2023, **472**, 144959.
24 A. Nikolaidis, T. Vouzara and E. Koulaouzidou, *Dent. Mater. J.*, 2020, **39**, 773–783.
25 Z. Shareh and M. Zamani, *Compos. Interfaces*, 2023, **30**, 1173–1200.
26 H. Ebrahimi, H. Roghani-Mamaqani and M. Salami-Kalajahi, *Polym. Bull.*, 2018, **75**, 4859–4880.
27 Y. Wang, J. Wang, Z. Ding, X. Cheng, R. Liu, J. Guo, H. Liu, L. Zong, X. Jian and J. Wang, *ACS Appl. Mater. Interfaces*, 2024, **16**, 68316–68327.
28 M. Han, Y. Zhang, Y. Zhang, Q. Ye, M. Sillanpää, X. Zhu and W. Yang, *Sustainable Chem. Pharm.*, 2024, **42**, 101861.
29 I. Rezaei and A. Sadeghi, *Arabian J. Sci. Eng.*, 2021, **46**, 12479–12486.
30 B. Aksoy, B. N. Altay, A. G. Teke and M. Demir, *Sci. Rep.*, 2025, **15**, 24200.

31 M. Tavassoli, B. Bahramian, R. Abedi-Firoozjah, N. Jafari, H. Javdani, S. M. Sadeghi, S. Hadavifar, S. Majnouni, A. Ehsani and S. Roy, *Food Bioprocess Technol.*, 2025, **18**, 3223–3244.
32 S. S. Alharthi, M. G. Althobaiti, A. A. Alkathiri, E. E. Ali and A. Badawi, *Taibah Univ. Sci*, 2022, **16**, 317–329.
33 S. Sakarkar, S. Muthukumaran and V. Jegatheesan, *Chemosphere*, 2020, **257**, 127144.
34 A. A. Oun, G. H. Shin, J.-W. Rhim and J. T. Kim, *Food Packag. Shelf Life*, 2022, **34**, 100991.
35 Y. Ning, W. Yang, S. Liu, J. Xu, X. Cheng, S. Xu, J. Li and L. Wang, *Adv. Funct. Mater.*, 2025, **35**, 2411314.
36 H. Deng, J. Su, W. Zhang, A. Khan, M. A. Sani, G. Goksen, P. Kashyap, P. Ezati and J.-W. Rhim, *Int. J. Biol. Macromol.*, 2024, **273**, 132926.
37 H. Abral, M. Ikhsan, D. Rahmadiawan, D. Handayani, N. Sandrawati, E. Sugiarti and A. N. Muslimin, *J. Mater. Res. Technol.*, 2022, **17**, 2193–2202.
38 M. Inagaki, Y. Hirose, T. Matsunaga, T. Tsumura and M. Toyoda, *Carbon*, 2003, **41**, 2619–2624.
39 H.-J. Kwon, S.-M. Hong, S.-M. Park and C. W. Lee, *Food Packag. Shelf Life*, 2024, **43**, 101271.
40 Z. Zhang, X. Zhang, B. Lin, Y. Zhong, W. Zhang, S. Zhong and X. Chen, *Food Chem.:X*, 2024, **24**, 102012.
41 S. Zhang, P. Sun, X. Lin, H. Wang, X. Huang, H. Liu and X. Xu, *Int. J. Biol. Macromol.*, 2025, **285**, 138076.
42 Z. Cheng, J. Li, G. He, M. Su, N. Xiao, X. Zhang, L. Zhong, H. Wang, Y. Zhong, Q. Chen, Y. Chen and M. Liu, *Int. J. Biol. Macromol.*, 2024, **280**, 136112.
43 E. Rynkowska, K. Fatyeyeva, S. Marais, J. Kujawa and W. Kujawski, *Polymers*, 2019, **11**, 1799.
44 Z. Cheng, M. Ning, K. Mao, X. Nong, J. Li, N. Xiao, X. Zhang, Q. Ding, H. Wang and M. Liu, *Int. J. Biol. Macromol.*, 2025, **316**, 144781.
45 Y.-W. Liu, Z.-S. Nong, T.-N. Man, S.-W. Lu and L.-H. Dong, *J. Mater. Res. Technol.*, 2024, **30**, 318–331.
46 S. Srinivasan, C. Ge, C. L. Lewis, S. S. Begum, A. B. Samui and H. F. Noyes, *Carbohydr. Polym.*, 2025, 124019.
47 J. Chen, P. Liu, J. Lu, S. Y. Jiang, C.-H. Lee, Y. Zhao, Y. Li and H. D. Ruan, *Mater. Chem. Phys.*, 2025, 131008.
48 L. Wei, P. Wang, X. Chen and Z. Chen, *Surf. Interfaces*, 2024, **52**, 104981.